RESEARCH ARTICLE | JULY 10 2023

The invariance and distortion of vectorial light across a real-world free space link

Cade Peters ; Mitchell Cox ; Alice Drozdov ; Andrew Forbes

Appl. Phys. Lett. 123, 021103 (2023)
https://doi.org/10.1063/5.0152065

Applied Physics Letters ARTICLE pubs.aip.org/aip/apl

The invariance and distortion of vectorial light across a real-world free space link

Cite as: Appl. Phys. Lett. **123**, 021103 (2023); doi: 10.1063/5.0152065
Submitted: 27 March 2023 · Accepted: 20 June 2023 ·
Published Online: 10 July 2023

Cade Peters,[1] Mitchell Cox,[2] Alice Drozdov,[2] and Andrew Forbes[1,a)]

AFFILIATIONS

[1]School of Physics, University of the Witwatersrand, Private Bag 3, Wits 2050, South Africa
[2]School of Electrical and Information Engineering, University of the Witwatersrand, Private Bag 3, Wits 2050, South Africa

[a)]Author to whom correspondence should be addressed: andrew.forbes@wits.ac.za

ABSTRACT

Vectorial structured light, where the polarization is inhomogeneously distributed in space, has found a myriad of applications in both 2D and 3D optical fields. Here, we present an experimental study of the invariance and distortion of vectorial light through a real-world medium of atmospheric turbulence. We show that the amplitude and polarization structure are both severely distorted by the turbulent medium, yet the non-separability of these two degrees of freedom remains invariant. We monitor this invariance under a range of beam types and atmospheric conditions, over extended time periods, revealing the unitary nature of atmospheric turbulence in our experiment. Our results provide conclusive evidence that invariance and distortion are not mutually exclusive and that the degree of classical entanglement remains unaltered through such channels, and will be of interest to the large community interested in classical and quantum communication in free space.

Optical systems form an integral part of our global communication infrastructure through guided and free space channels, allowing for the rapid and reliable transfer of information. Free space optical links have received renewed interest in recent years, with so-called structured light[1] fueling a significant increase in the number of available channels and an increase in the capacity per channel,[2,3] with orbital angular momentum (OAM) modes arguably the most popular choice for the encoding alphabet.[4,5] Tailoring light's spatial degrees of freedom therefore presents an excellent toolbox for the improvement of optical channels and offers a promising and relatively accessible way to bridge the digital divide.[6] Unfortunately atmospheric turbulence results in distorted beams and modal crosstalk at the receiver,[7] which has significantly hindered the reach, with the state-of-the-art of gigabit-per-second communication with OAM limited to a 260 m free space channel.[8]

Vectorial light, which has already found applications in both classical[9,10] and quantum[11–14] free space links, has been put forward as a potential solution to this problem due to the apparent robustness of the polarization degree of freedom (DoF). Vector modes are formed by combining two spatial modes, each in an orthogonal polarization state to create exotic, inhomogeneous polarization structures. Studies of vector OAM beams through random media have reported robustness,[15–17] while others reported no advantage beyond that of scalar OAM modes.[18–21] A quantum-inspired study has revealed that the non-separability of DoFs is the only invariant quantity,[22] but so far has been tested only in single sided channels in the laboratory.

Here, we report results showing the modal distortion and non-separability invariance of vectorial light across a real-world free space link. The tests were done over a 270 m path of varying atmospheric turbulence conditions and using a variety of vectorial modes. We find that the amplitude and polarization structure of vectorial light is not robust and can in fact be significantly aberrated, but that the non-separability is invariant. We test this invariance over an extended period of time and across many different conditions, validating the assumption of the unitary nature of our atmospheric channel and opening a path to its exploitation for distortion-free forms of light[23] or lossless pre- and post-correction techniques.[24,25] In addition to reporting on a powerful toolbox for probing complex channels with vectorial light, our work will be of value to those interested in pursuing robust optical communication across noisy channels.

We first construct vector light fields of the following form:

$$|\Psi\rangle = \sqrt{a}|\psi_+\rangle|H\rangle + \sqrt{1-a}|\psi_-\rangle|V\rangle, \quad (1)$$

where $|\psi_\pm\rangle$ are any two orthogonal spatial modes, $|H(V)\rangle$ are the horizontal (vertical) polarization Jones matrices, and a is a weighting

factor ensuring that the field's total power remains constant for $a \in [0, 1]$. These fields have a degree of non-separability between their spatial and polarization degrees of freedom, which can be captured using a quantum-inspired metric known as the concurrence or vector quality factor,[26] quantifying how inhomogeneous the polarization structure is (1 for perfectly vector and 0 for scalar fields), given by

$$\mathscr{C} = 2\sqrt{\langle\psi_+|\psi_+\rangle\langle\psi_-|\psi_-\rangle + |\langle\psi_+|\psi_-\rangle|^2}, \tag{2}$$

which simplifies to $\mathscr{C} = 2|\sqrt{a(1-a)}|$ for beams in the form of Eq. (1). Equation (2) gives the concurrence solely in terms of inner products between the two orthogonal spatial modes $|\psi_\pm\rangle$ and is, therefore, invariant under any transformation that preserves inner products, e.g., unitary operations. Thus, the concurrence will be preserved if it propagates through a unitary channel, even if that channel is noisy atmospheric turbulence. It is a statement that the modal information may appear distorted, but the degree of non-separability will remain invariant. This concept is captured schematically in Fig. 1. Vectorial modes using OAM as the spatial basis, as illustrated in Fig. 1(a), are created by changing the weighting parameter a, thus changing the degree of non-separability, $\mathscr{C}$, and the homogeneity of the polarization structure. Each vectorial mode (four examples shown) is passed through a turbulent channel, as seen in Fig. 1(b) and measured at the output, as illustrated in Fig. 1(c), where we predict a distortion in the spatial structure but an invariance in the degree of non-separability. Till now, we have considered orthogonal spatial modes, but this is not necessary for the concurrence to remain invariant. It has been shown that for any arbitrary vectorial light field

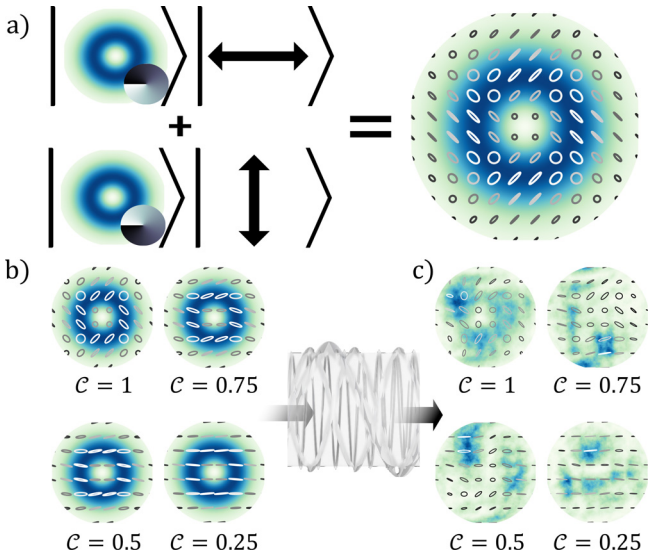

FIG. 1. The invariance of vector modes. (a) The concurrence of a vector mode can be chosen by modulating the relative amplitudes a between two orthogonal spatial modes. (b) These spatial modes may then be superimposed when orthogonally polarized to form a vector beam with the chosen concurrence. (c) When these beams pass through a turbulent channel (simulated in the above-mentioned figure), the amplitude and polarization structure will be severely aberrated, but the encoded concurrence value will remain invariant.

$$|\Phi\rangle = |\tilde{\phi}_h\rangle|H\rangle + |\tilde{\phi}_v\rangle|V\rangle, \tag{3}$$

where $|\tilde{\phi}_{h(v)}\rangle$ are any two arbitrary spatial states; one can write the concurrence as[27]

$$\mathscr{C}(|\Phi\rangle) = 2\sqrt{\langle\tilde{\phi}_h|\tilde{\phi}_h\rangle\langle\tilde{\phi}_v|\tilde{\phi}_v\rangle - |\langle\tilde{\phi}_h|\tilde{\phi}_v\rangle|^2}. \tag{4}$$

In this equation, we see that the concurrence depends solely on the inner products between the two arbitrary spatial states $|\tilde{\phi}_{h(v)}\rangle$. The concurrence of a vector mode made up of two arbitrary spatial states should then be invariant to any unitary operation. It is important to keep on mind that even though we have studied vector modes made of orthogonal spatial states in this work, the conclusions should then hold for any vector beam made up of arbitrary spatial states, including highly asymmetric combinations of modes.[28]

Our experiment is shown in Fig. 2(a) and comprises of generation, propagation, and detection stages. In the generation stage, a collimated and expanded green diode laser ($\lambda = 520$ nm) was directed onto a reflective PLUTO-VIS (HoloEye) spatial light modulator (SLM). The screen of this SLM was divided into two halves. Each half was encoded with the desired scalar mode (e.g., two Laguerre–Gaussian beams with $\ell = \pm 1$, one on each half). In order to create a vector mode, the two beams were combined using a Mach–Zehnder interferometer. This was done by first passing one of the scalar modes through a half-wave plate (HWP) with the fast axis at an angle of 45°, converting it from horizontal to vertical polarization. The two beams were then combined using a polarizing beam splitter (PBS). The vector beam was then propagated through a 270 m turbulence free space link before being sent to the detection stage. Due to the rapidly changing nature of atmospheric turbulence, it was necessary to capture all the polarization projections of the vector beam simultaneously. To achieve this, the incoming vector beam was passed through a 50:50 beam splitter (BS). One arm of the BS was incident directly onto a Mako G-508 polarization-sensitive camera, which is capable of measuring all four linear polarization states simultaneously. The circularly polarized components were measured by passing the other arm of the BS through a quarter-wave plate (QWP) with its fast axis at an angle of 45°. This converted the right-circularly and left-circularly polarized components to horizontal and vertical polarizations, respectively. This arm was then incident on the same camera, although in a different position on the sensor, allowing for the circular polarization components to be measured. The simultaneously captured images of each polarization projection from the camera are shown in Fig. 2(b). The camera's frame capture time was 2 ms, far faster than the turbulence coherence time of order 10–100 ms, ensuring that all polarization projections experienced the same turbulence conditions.

The concurrence for each frame was then calculated from[27] as

$$\mathscr{C} = \sqrt{1 - \frac{P_1^2 + P_2^2 + P_3^2}{P_0^2}}, \tag{5}$$

where

$$P_i = \int_{-\infty}^{\infty}\int_{-\infty}^{\infty} S_i(\vec{r})\mathrm{d}A \tag{6}$$

and $S_i(\vec{r})$ is the relevant spatially resolved Stokes parameter. To ensure that the detection system worked accurately, it was first tested in a

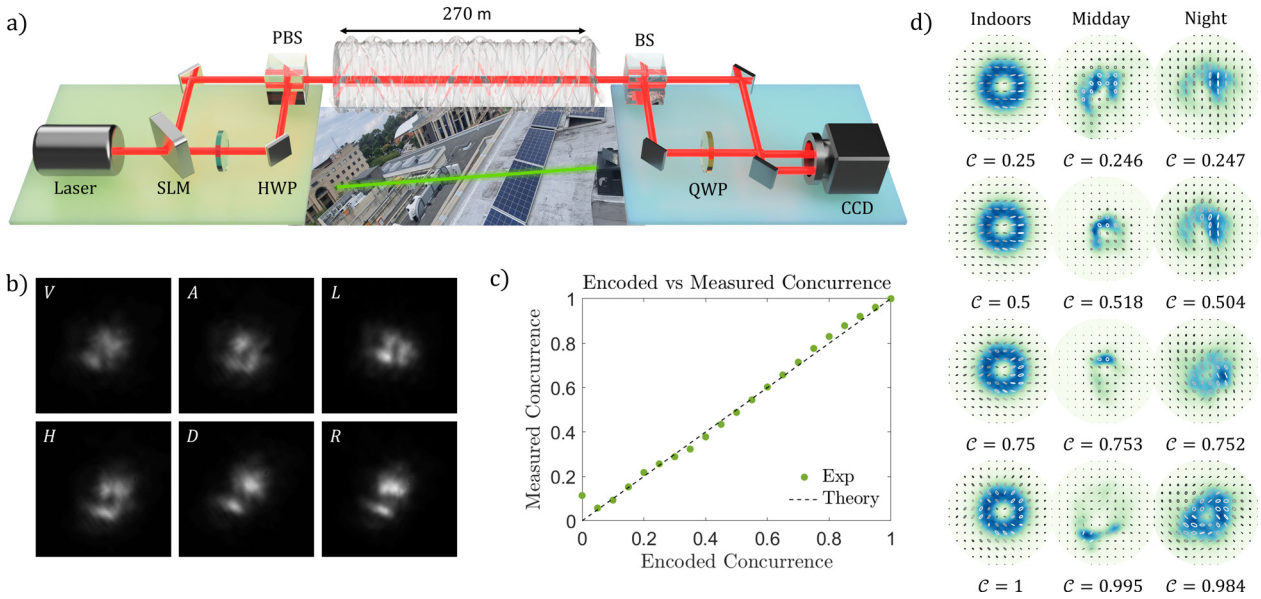

FIG. 2. Experimental setup. (a) A vector mode with a chosen concurrence is generated by encoding two orthogonal spatial modes onto an SLM. These horizontally polarized spatial modes are then combined using a Mach–Zehnder interferometer. This mode is subsequently sent through a 270 m real-world free space optical link before arriving at a detector. The detector splits the beam evenly using a beam splitter and directs one arm to a polarizer camera. The other arm is passed through a QWP before being directed onto the same camera allowing for all six polarization projections of the beam to be captured simultaneously. (b) The captured image of each polarization projection of the vector beam after passing through the free space link. (c) Plot showing the encoded vs measured concurrence of a vector beam in a controlled indoor + laboratory setting. (d) The amplitude and polarization structure of several vector beams with the encoded concurrence of $\mathscr{C} = 0.25, 0.5.0.75$, and 1 for conditions of Indoors (within the laboratory), Midday (noon), and Night (after sunset). The measured concurrence averaged over all three instances (Indoors, Midday, and Night) is 0.248 ± 0.13, 0.507 ± 0.06, 0.752 ± 0.04, and 0.993 ± 0.03, respectively. Both the amplitude and polarization structure is severely aberrated, but the concurrence remains invariant.

controlled laboratory setting without sending the beam through the free space link. The results of this loopback test in Fig. 2(c) show that the measured and encoded concurrences are in very close agreement, as can be seen from the nearly perfect straight line fit. This confirms that the creation and detection stages were highly accurate and effective.

Example experimental results for four different vectorial beams of concurrences $\mathscr{C} = 0.25, 0.5, 0.75$, and 1 are shown in Fig. 2(d). In these tests, the vectorial beams were constructed from the LG basis with OAM values of $\ell = \pm 1$, with single snapshots shown for test conditions of Indoors (for benchmarking) as well as across the 270 m link at Midday and Night time. Upon comparison, one can see that the amplitude structure is significantly distorted, as would be expected due to atmospheric turbulence, as too is the polarization structure. The examples shown are exemplary of the type of distortion observed, confirming that the spatially varying polarization structure is not robust against atmospheric turbulence.

Next, we measured the concurrence as a function of time: every minute for a period of two hours between 18h00 and 20h00 during sunset. Every minute, a beam with a specified concurrence was sent through the link and ten measurements were taken over a period of five seconds. The averaged results of these experiments are shown in Fig. 3(a), with the standard deviation shown as the error bars. The average scintillation index of atmosphere was $\sigma_I^2 = 0.25$ during the measurement period. The transmitted power in each beam was normalized so that the same total power was transmitted irrespective of the encoded concurrence. For the higher encoded values of concurrence ($\mathscr{C} = 0.5, 0.75$, and 1), it is clear that the value remains constant throughout the two hour period with only slight fluctuations around the encoded value. For $\mathscr{C} = 0.25$, we do see some noticeable fluctuations, with the encoded concurrence still within the standard deviation. More erratic behavior is to be expected at lower values due to the very low relative intensity of one of the orthogonally polarized spatial modes. The intensity of the lower weighted mode is very close to the noise floor, making it more difficult to filter out and determine accurately.

Figure 3(b) shows a more dynamic view of the concurrence through the channel by zooming into a time interval of 45 s showing the individual measured values every second. The value is relatively stable about the encoded value with periods of highly erratic behavior and periods of stable behavior. The source of the fluctuations can be attributed to several factors, including alignment drifts (pointing errors), and possibly slight deviations from unitarity, e.g., scattering and absorption of light by aerosols and other particles suspended in the atmosphere. This causes light to be lost or directed away from the detector, thus altering the measured value of the concurrence.

Finally, it has been suggested that some types of polarization structures are more robust than others.[15] To test this, we alter the OAM basis from the prior tests with $\ell = \pm 1$ (V-point singularity) to a superposition of $\ell = 0$ and $\ell = 1$ (C-point singularity), with the results shown in Fig. 4. The main panel shows the accumulated variance over 2 h for both polarization structures (C-point and V-point), with the inset showing an example of a received and distorted C-point beam. We find that over the measurement period, the variances in the

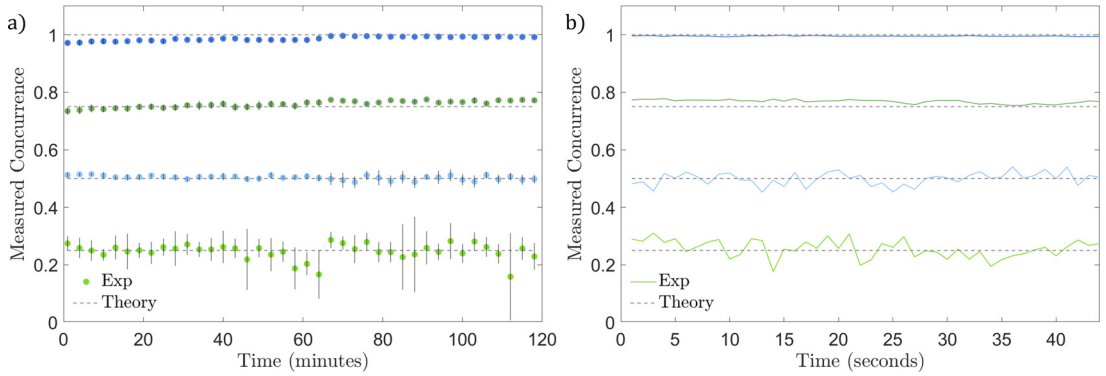

FIG. 3. Concurrence over time. (a) Plot showing the average measured concurrence values of a vector beam constructed in Laguerre–Gaussian (LG) basis with OAM values of $\ell = \pm 1$ with encoded concurrences $\mathscr{C} = 0.25, 0.5.0.75$, and 1 over a period of 2 h from 18h00 to 20h00. This covers the period of sunset, which occurred around 19h00 on the day of the measurements. The plot shows the average value for each set of ten measurements with the error bars indicating the standard deviation of the set. (b) Plot showing the exact measured value of the concurrence every second.

concurrence of both the C-point and V-point beam are comparable. This suggests that neither singularity type provides greater stability to the concurrence of the vector beam. Comparing 400 measurements taken for each singularity type encoded with a concurrence of 0.75, a two sample F-test for equal variance in the concurrence was performed. This test showed with a 95% confidence that the variance between both beam types is comparable, suggesting that neither singularity holds significant advantages over the other.

From our results, we can conclude that vectorial light is distorted in atmospheric turbulence, but that the non-separability is invariant. This is corroborated by the many other beam types and beam orders that reveal the same behavior as the indicative results shown in this report. Since the non-separability of light is directly related to its classical entanglement,[29,30] we can state that the degree of classical entanglement remains unperturbed across varying beam types and turbulence conditions. Methods for overcoming the effects of atmospheric turbulence remain an important and pressing challenge. Here, using the spatial and polarization degrees of freedom, we have demonstrated the distortion and invariance of the non-separability of vectorial light through a 270 m real-world free space link. Our demonstration provides evidence for the invariance of the non-separability of vectorial light through real-world channels and the unitary nature of our atmospheric turbulence channel.

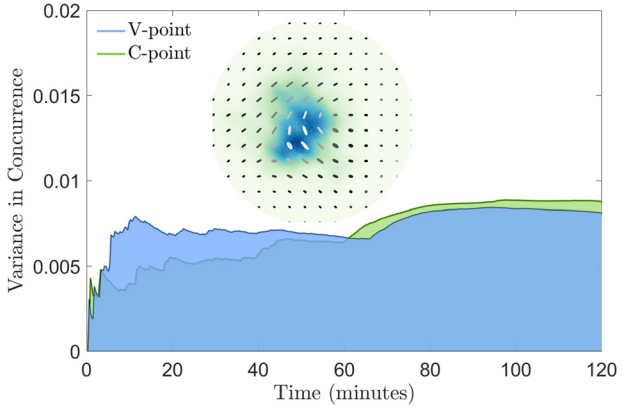

FIG. 4. Polarization singularities. The plot shows the cumulative variance of a C-point and V-point beams. The plot shows the variance of the concurrence as each new data point is measured and included in the data set. The inset shows the intensity and polarization structure of the C-point beam after it has passed through the free space link.

C. Peters and A. Forbes acknowledge the funding from the National Research Fund (NRF).

AUTHOR DECLARATIONS

Conflict of Interest

The authors have no conflicts to disclose.

Author Contributions

Cade Ribeiro Peters: Data curation (equal); Formal analysis (equal); Investigation (equal); Methodology (equal); Resources (equal); Writing – original draft (equal); Writing – review & editing (equal). **Mitchell Arij Cox:** Resources (equal); Supervision (equal); Writing – review & editing (equal). **Alice Vadimovna Drozdov:** Data curation (equal); Investigation (supporting); Methodology (supporting); Writing – review & editing (equal). **Andrew Forbes:** Conceptualization (equal); Data curation (equal); Funding acquisition (equal); Project administration (equal); Resources (equal); Supervision (equal); Writing – review & editing (equal).

DATA AVAILABILITY

The data that support the findings of this study are available from the corresponding author upon reasonable request.

REFERENCES

[1]A. Forbes, M. de Oliveira, and M. R. Dennis, "Structured light," Nat. Photonics **15**, 253–262 (2021).
[2]A. Trichili, K.-H. Park, M. Zghal, B. S. Ooi, and M.-S. Alouini, "Communicating using spatial mode multiplexing: Potentials, challenges, and perspectives," IEEE Commun. Surv. Tutorials **21**, 3175–3203 (2019).

[3]G. Li, N. Bai, N. Zhao, and C. Xia, "Space-division multiplexing: The next frontier in optical communication," Adv. Opt. Photonics **6**, 413–487 (2014).
[4]M. J. Padgett, "Orbital angular momentum 25 years on," Opt. Express **25**, 11265–11274 (2017).
[5]A. E. Willner, H. Huang, Y. Yan, Y. Ren, N. Ahmed, G. Xie, C. Bao, L. Li, Y. Cao, Z. Zhao, J. Wang, M. P. J. Lavery, M. Tur, S. Ramachandran, A. F. Molisch, N. Ashrafi, and S. Ashrafi, "Optical communications using orbital angular momentum beams," Adv. Opt. Photonics **7**, 66–106 (2015).
[6]M. P. Lavery, M. M. Abadi, R. Bauer, G. Brambilla, L. Cheng, M. A. Cox, A. Dudley, A. D. Ellis, N. K. Fontaine, A. E. Kelly *et al.*, "Tackling Africa's digital divide," Nat. Photonics **12**, 249–252 (2018).
[7]M. A. Cox, N. Mphuthi, I. Nape, N. Mashaba, L. Cheng, and A. Forbes, "Structured light in turbulence," IEEE J. Sel. Top. Quantum Electron. **27**, 7500521 (2021).
[8]Y. Zhao, J. Liu, J. Du, S. Li, Y. Luo, A. Wang, L. Zhu, and J. Wang, "Experimental demonstration of 260-meter security free-space optical data transmission using 16-QAM carrying orbital angular momentum (OAM) beams multiplexing," in *Optical Fiber Communications Conference and Exhibition (OFC)* (IEEE, 2016), pp. 1–3.
[9]G. Milione, M. P. J. Lavery, H. Huang, Y. Ren, G. Xie, T. A. Nguyen, E. Karimi, L. Marrucci, D. A. Nolan, R. R. Alfano, and A. E. Willner, "4 Gbit/s mode division multiplexing over free space using vector modes and a *q*-plate mode (de)multiplexer," Opt. Lett. **40**, 1980–1983 (2015).
[10]Z. Zhu, M. Janasik, A. Fyffe, D. Hay, Y. Zhou, B. Kantor, T. Winder, R. W. Boyd, G. Leuchs, and Z. Shi, "Compensation-free high-dimensional free-space optical communication using turbulence-resilient vector beams," Nat. Commun. **12**, 1666 (2021).
[11]I. Nape, N. Mashaba, N. Mphuthi, S. Jayakumar, S. Bhattacharya, and A. Forbes, "Vector-mode decay in atmospheric turbulence: An analysis inspired by quantum mechanics," Phys. Rev. Appl. **15**, 034030 (2021).
[12]A. Sit, F. Bouchard, R. Fickler, J. Gagnon-Bischoff, H. Larocque, K. Heshami, D. Elser, C. Peuntinger, K. Günthner, B. Heim, C. Marquardt, G. Leuchs, R. W. Boyd, and E. Karimi, "High-dimensional intracity quantum cryptography with structured photons," Optica **4**, 1006–1010 (2017).
[13]I. Nape, E. Otte, A. Vallés, C. Rosales-Guzmán, F. Cardano, C. Denz, and A. Forbes, "Self-healing high-dimensional quantum key distribution using hybrid spin-orbit bessel states," Opt. Express **26**, 26946–26960 (2018).
[14]B. Ndagano, I. Nape, M. A. Cox, C. Rosales-Guzman, and A. Forbes, "Creation and detection of vector vortex modes for classical and quantum communication," J. Lightwave Technol. **36**, 292–301 (2018).
[15]P. Lochab, P. Senthilkumaran, and K. Khare, "Designer vector beams maintaining a robust intensity profile on propagation through turbulence," Phys. Rev. A **98**, 023831 (2018).
[16]Y. Gu, O. Korotkova, and G. Gbur, "Scintillation of nonuniformly polarized beams in atmospheric turbulence," Opt. Lett. **34**, 2261–2263 (2009).
[17]W. Cheng, J. W. Haus, and Q. Zhan, "Propagation of vector vortex beams through a turbulent atmosphere," Opt. Express **17**, 17829–17836 (2009).
[18]M. A. Cox, C. Rosales-Guzmán, M. P. Lavery, D. J. Versfeld, and A. Forbes, "On the resilience of scalar and vector vortex modes in turbulence," Opt. Express **24**, 18105–18113 (2016).
[19]Y. Cai, Q. Lin, H. T. Eyyuboğlu, and Y. Baykal, "Average irradiance and polarization properties of a radially or azimuthally polarized beam in a turbulent atmosphere," Opt. Express **16**, 7665–7673 (2008).
[20]P. Ji-Xiong, W. Tao, L. Hui-Chuan, and L. Cheng-Liang, "Propagation of cylindrical vector beams in a turbulent atmosphere," Chin. Phys. B **19**, 089201 (2010).
[21]T. Wang and J. Pu, "Propagation of non-uniformly polarized beams in a turbulent atmosphere," Opt. Commun. **281**, 3617–3622 (2008).
[22]I. Nape, K. Singh, A. Klug, W. Buono, C. Rosales-Guzman, A. McWilliam, S. Franke-Arnold, A. Kritzinger, P. Forbes, A. Dudley *et al.*, "Revealing the invariance of vectorial structured light in complex media," Nat. Photonics **16**, 538–546 (2022).
[23]A. Klug, C. Peters, and A. Forbes, "Robust structured light in atmospheric turbulence," Adv. Photonics **5**, 016006 (2023).
[24]C. He and M. J. Booth, "Vectorial adaptive optics: Correction of polarization and phase," in *Adaptive Optics and Applications* (Optica Publishing Group, 2022), p. OTh3B–4.
[25]Y. Ren, G. Xie, H. Huang, N. Ahmed, Y. Yan, L. Li, C. Bao, M. P. Lavery, M. Tur, M. A. Neifeld *et al.*, "Adaptive-optics-based simultaneous pre-and post-turbulence compensation of multiple orbital-angular-momentum beams in a bidirectional free-space optical link," Optica **1**, 376–382 (2014).
[26]M. McLaren, T. Konrad, and A. Forbes, "Measuring the nonseparability of vector vortex beams," Phys. Rev. A **92**, 023833 (2015).
[27]A. Selyem, C. Rosales-Guzmán, S. Croke, A. Forbes, and S. Franke-Arnold, "Basis-independent tomography and nonseparability witnesses of pure complex vectorial light fields by stokes projections," Phys. Rev. A **100**, 063842 (2019).
[28]C. Samlan and N. K. Viswanathan, "Generation of vector beams using a double-wedge depolarizer: Non-quantum entanglement," Opt. Lasers Eng. **82**, 135–140 (2016).
[29]Y. Shen and C. Rosales-Guzmán, "Nonseparable states of light: From quantum to classical," Laser Photonics Rev. **16**, 2100533 (2022).
[30]A. Forbes, A. Aiello, and B. Ndagano, "Classically entangled light," in *Progress in Optics* (Elsevier, 2019), Vol. 64, pp. 99–153.